Asian Journal of Chemistry; Vol. 26, No. 23 (2014), 8173-8180

ASIAN JOURNAL OF CHEMISTRY

http://dx.doi.org/10.14233/ajchem.2014.17770

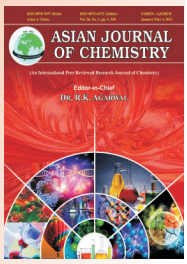

Removal of Cu(II) from Water Environment Using Lignocellulose/ Montmorillonite Nanocomposite-An Industrial Waste Adsorbent

XIAOTAO ZHANG[1] and XIMING WANG[2,*]

[1]College of Science, Inner Mongolia Agricultural University, Hohhot 010018, P.R. China
[2]College of Material Science and Art Design, Inner Mongolia Agricultural University, Hohhot 010018, P.R. China

*Corresponding author: Fax: +86 471 4313037; Tel: +86 138 04711097; E-mail: lianzixiaotao@163.com

Received: 10 April 2014; *Accepted*: 7 June 2014; *Published online*: 15 November 2014; AJC-16320

The lignocellulose/montmorillonite nanocomposite was taken as adsorbent to investigate the adsorption and desorption properties of Cu(II) in copper-contained wastewater, which was synthesized by the chemical intercalation process of lignocellulose and montmorillonite. The affecting parameters on the Cu(II) removal rate by changing initial concentration of Cu(II), solution pH, adsorption temperature and adsorption time were studied. The equilibrium adsorption capacity could reach 322.56 mg g^{-1} under the optimal condition, *i.e*., 0.03 mol L^{-1} initial concentration of Cu(II) ion, 4.9 is the solution pH, 50 ºC is the adsorption temperature and 60 min is the adsorption time. The pseudo-second order kinetic model can well describe the whole adsorption process and the isotherm adsorption equilibrium conformed to the Langmuir model. The adsorption mechanism of lignocellulose/montmorillonite was discussed in combination with the results of SEM and FTIR. And then lignocellulose/montmorillonite could be easily eluted by HNO_3, the effects of HNO_3 concentration, desorption temperature and desorption time on desorption capacity of lignocellulose/montmorillonite were tested. The results showed that HNO_3 concentration 0.1 mol L^{-1}, desorption temperature 40 ºC and desorption time 0.5 h, the satisfactory effect of desorption capacity was 283.15 mg g^{-1}. The adsorption/desorption experiment displayed that the adsorption capacity of lignocellulose/montmorillonite was ideal for four cycles, so lignocellulose/montmorillonite is confirmed a high efficient adsorbent for recycling.

Keywords: Lignocellulose, Montmorillonite, Nanocomposite, Cu(II), Adsorption, Desorption, Wastewater.

INTRODUCTION

Water contamination caused by heavy metal ions from metallurgy, printing, paper, rubber, plastic and electronics industries, *etc*., is a global problem that has received worldwide concern[1,2]. Among the numerous heavy metals, which is significantly toxic to human beings and ecological environment, Cu(II) is one of the most common pollutants found in industrial effluents. Even though the high economic value of Cu(II)-contained wastewater, its potential harmfulness have carcinogenic and mutagenic effects that lead to critical health problems. Traditional technologies for the removal of Cu(II), such as ion exchange, chemical precipitation, biological treatment, reverse osmosis and electrochemical processes have been used for the reduction of Cu(II) at very low concentration, but these approaches are commercially impractical because of lack of cost effectiveness, versatility, ease of integration, *etc*. Hence, adsorption is an effective technique with the advantages of high efficiency even from dilute concentrations, minimization of secondary wastes and low cost. Due to economic considerations, natural polymeric materials[3] are gaining interest for application as adsorbents in wastewater treatment.

Lignocellulose, is known as an ideal natural adsorbent[4] for the removal of heavy metal ions[5] because of its specific characteristics[6]. Lignocellulose is a renewable polymer, existing widely in plant seeds, which is primarily composed of cellulose, hemicellulose and lignin[7]. Moreover, a variety of reactive functional groups exist in its three-dimensional structure, including phenolic, hydroxyl, carboxyl and other active groups, which can be used as active adsorption sites for heavy metal ions[8-10]. However, because of its polydispersity properties and amorphous structure, lignocellulose is not suitable to be applied extensively.

Recently, clay have been accepted as one of the most appropriate low-cost adsorbents for the removal of heavy metal ions from wastewater. Among the clays studied, montmorillonite is a kind of silicate minerals with nanolamellar structures[11], however, because of little affinity, swelling and dispersed suspension properties in water, montmorillonite adsorbed heavy metal ions only onto the external broken-bonds surface in very small amounts. Therefore, in order to improve the adsorption capacities for heavy metal ions, chemical modification of montmorillonite are expected to show higher adsorption capacities than common clay minerals.

To our best of knowledge, there is rarely no literature focusing on the adsorption capacity of Cu(II) by using a lignocellulose/montmorillonite nanocomposite[12]. So, novel lignocellulose/montmorillonite nanocomposite has been prepared in this work. Furthermore, its adsorption and desorption capacities for Cu(II) have been observed. Each adsorption and desorption influencing factors, including initial concentration of Cu(II), pH, adsorption temperature, adsorption time, concentration of HNO_3, desorption temperature and desorption time, have been investigated. Furthermore, the adsorption kinetics and isotherms onto lignocellulose/montmorillonite were studied and the mechanism of Cu(II) adsorption was discussed. Finally, exploratory research results on the recycling application of lignocellulose/montmorillonite nanocomposite offered a reference for Cu(II) removal and its regeneration ability was evaluated through four adsorption/desorption cycles and showed a good recycling.

EXPERIMENTAL

Lignocellulose (SAM-100), obtained from Beijing Huaduo Biotech Ltd., China. Montmorillonite [CEC = 100 meq (100 g^{-1})], purchased from Zhejiang Feng Hong Clay Chemical Co., China, was ground and sieved to 200 mesh size. $CuSO_4$, obtained from Shanghai Jinshan Chemical Co. China, was used to prepared the adsorbate solution. Other agents used were analytic grade without further purification. All solutions were prepared with distilled water.

Micrographs of the samples were taken by scanning electron microscopy (SEM) (JSM-5600LV, JEOL, Tokyo, Japan). Before observation of SEM, all samples were fixed on aluminum stubs and coated with gold. FTIR spectra of samples were characterized by using a FTIR Spectrophotometer (Thermo Nicolet NEXUS, TM) in KBr pellets.

Preparation of lignocellulose/montmorillonite nanocomposite: The nanocomposite were prepared by the method of Wang and Pang[13]. A certain amount of lignocellulose was dissolved in NaOH solution [weight of lignocellulose (g): volume of NaOH (mL) = 1:30] in batches, after magnetically stirred, forming a uniform lignocellulose suspension. And then a suspension of montmorillonite (1 g suspended in 30 mL of distilled water) was stirred (500 rpm) for 0.5 h, followed by the addition of the lignocellulose-NaOH suspension. It was heated to 60 °C with stirring for 6 h. The reaction mixtures were centrifuged and washed with an acid solution until the pH of the supernatant reached 7. After that, vacuum dried at 105 °C (DZF-6210) for 5 h until the weight was stable. All samples were ground and sieved to 200 mesh size. The density of the samples was measured by stack density methods.

Adsorption experiment: An amount of lignocellulose/montmorillonite 0.1000 g (BS210S) was accurately weighted and added into 50 mL Cu(II) solution with a measured concentration. The suspension was stirred at a uniform speed of 120 rpm in a thermostatic shaker (SHA-C) and adjusted pH with a certain amount of CH_3COONa-CH_3COOH solution using a pH meter (PB-10). When the adsorption equilibrium was reached, the mixture was centrifuged at 6000 rpm for 10 min. The upper fluid was taken to determine the residual concentration of Cu(II) by an EDTA titrimetric method[14] using 0.05 M EDTA solution as a standard solution and 0.2 % xylenol orange solution as an indicator. The adsorption experiments were carried out in different Cu(II) initial concentrations, pH, adsorption temperature and adsorption time. Taking into account the experimental errors, three experiments were run in parallel under the same conditions and the obtained results were based on the average values. The adsorption capacity of Cu(II) solution was measured from the following equation:

$$q_{t,1} = \frac{(C_0 - C_{t,1})V_1 \times 63.5}{m_1} \quad (1)$$

where $q_{t,1}$ (mg g^{-1}) refers to the capacity of adsorption at time t (min). C_0 and $C_{t,1}$ (mol L^{-1}) refer to the Cu(II) initial concentration and final concentration at time t (min), respectively. V_1 (mL) refers to the volume of Cu(II). m_1(g) is the mass of adsorbent. In the method of calculating $q_{t,1}$, no losses of Cu(II) ions to any other mechanism (volatilization, sorption to the glassware, degradation, *etc*.,) were assumed.

Desorption and regeneration experiments: 0.1000 g Cu(II)-loaded lignocellulose/montmorillonite nanocomposite was accurately weighted and transferred into 50 mL HNO_3 solution with different concentrations. The mixture was put in an ultrasonic cleaning machine (KS-300EI). When the desorption equilibrium was reached at a certain temperature, the suspension was centrifuged, determining the concentrations of the desorbed Cu(II) solution. Taking into account the experimental errors, three experiments were performed and the reproducibility of the results was within ± 3 %. The desorption capacity of the Cu(II)-loaded lignocellulose/montmorillonite was calculated according to the following equation[15,16].

$$q_{t,2} = \frac{C_{t,2} V_2 \times 63.5}{m_2} \quad (2)$$

where $q_{t,2}$ (mg g^{-1}) refers to the desorption amount at time t (min). $C_{t,2}$ (mol L^{-1}) refers to the concentration of Cu(II) in the desorbed solution at time t (min). V_2 (mL) refers to the total volume of solution in desorption m_2 (g) refers to the mass of the adsorbent after adsorption of Cu(II).

Repeated batch experiments were performed to examine the reusability of lignocellulose/montmorillonite for Cu(II). The formed composites were washed with distilled water to remove the remaining acid and were dried in an oven (DZF-6210) at 70 ºC for the next adsorption of Cu(II). The adsorption and desorption capacities of Cu(II) were determined and analyzed. The consecutive adsorption/desorption process was performed five times.

RESULTS AND DISCUSSION

Effect of initial concentration of Cu(II) on adsorption: The effects of different Cu(II) initial concentrations on lignocellulose/montmorillonite adsorption capacity are shown in Fig. 1. It can be seen that the adsorption capacity trend of the lignocellulose/montmorillonite nanocomposite towards Cu(II) first increased and then remained stable when the Cu(II) initial concentration was increased. This is likely because of an increase in the amount of Cu(II) ions, which leads to the increase of collision times between Cu(II) ions and the active adsorption sites on lignocellulose/montmorillonite. Hence,

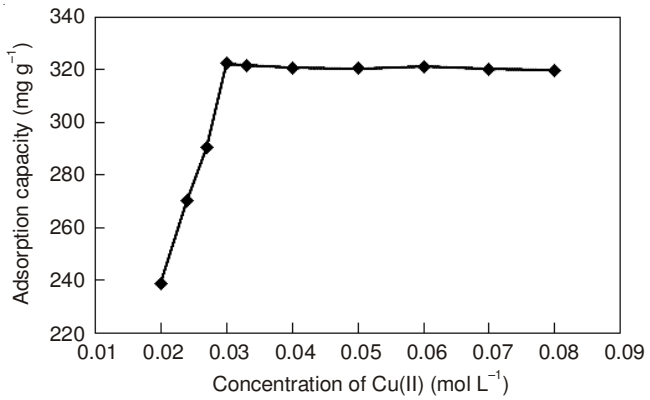

Fig. 1. Effect of Cu(II) initial concentration on adsorption capacity of lignocellulose/montmorillonite nanocomposite

increasing adsorption capacity. When Cu(II) concentration was further increased, the adsorption capacity remained stable due to the saturation of active adsorption sites. Therefore, Cu(II) with an initial concentration of 0.03 mol L^{-1} was chosen as the ideal initial concentration condition.

Effect of pH value on adsorption: The pH value of the Cu(II) solution is an important factor for the determination the adsorption of solutes. The influence of pH value on lignocellulose/montmorillonite adsorption capacity are shown in Fig. 2. This result indicated that the trend on adsorption capacity of lignocellulose/montmorillonite of Cu(II) exhibited an increase at first, followed by a decrease with the increasing of the pH. When pH was 4.9, adsorption capacity reached the maximum amount of 322.6 mg g^{-1}. This result can be accounted for as follows, when the pH was less than 4.9, the main reactive functional groups in lignocellulose/montmorillonite were -COOH and -OH, Cu(II) sorption through exchange of ions is favored at low pH values especially when the sorption rate is largely controlled by ion exchange rather than by complexation. As the pH increased, the anion group concentration ($-COO^-$) increased, the Cu(II) complexing ability with lignocellulose/montmorillonite was gradually increased. However, when the pH was higher than 4.9, Cu(II) could react with basic pH regulator, which resulted in facile complexation or precipitation and therefore a reduction in adsorption capacity[17]. It can be determined that the optimum pH for adsorption is 4.9.

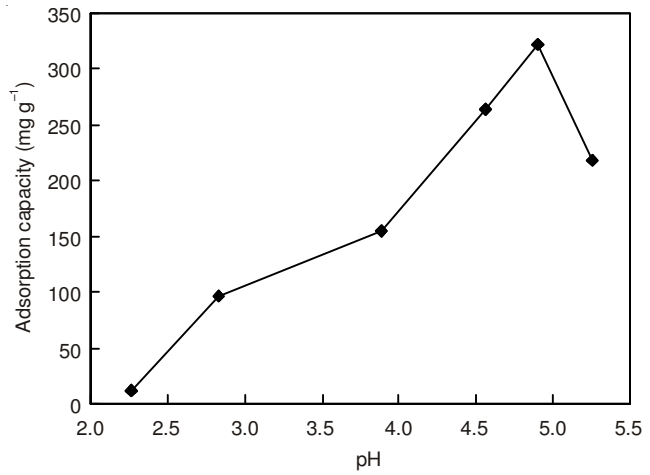

Fig. 2. Effect of pH on adsorption capacity of lignocellulose/montmorillonite nanocomposite

Effect of temperature on adsorption: Fig. 3 shows the relationship between the different temperatures and the adsorption capacity of Cu(II) by lignocellulose/montmorillonite nanocomposite. It can be seen that the adsorption capacity towards Cu(II) first increased and then dropped with a rise in temperature. This result is likely attributed to the enhanced activity of the lignocellulose/montmorillonite molecules with an increase in adsorption temperature, which is caused by the disruption of intermolecular hydrogen bonding interactions between the molecular chains with the acceleration of molecular thermal motion. With the increased number of activated molecules, the interaction between Cu(II) and the lignocellulose/montmorillonite was also enhanced, which was conducive to increase the absorption capacity. However, continued heating was shown to lead to decomposition of the lignocellulose/montmorillonite, with damage to the three-dimensional structures. It is found that the higher temperature is to the advantage of adsorption and the adsorption is an endothermic reaction. Therefore, an adsorption temperature of 50 °C was chosen as the ideal condition.

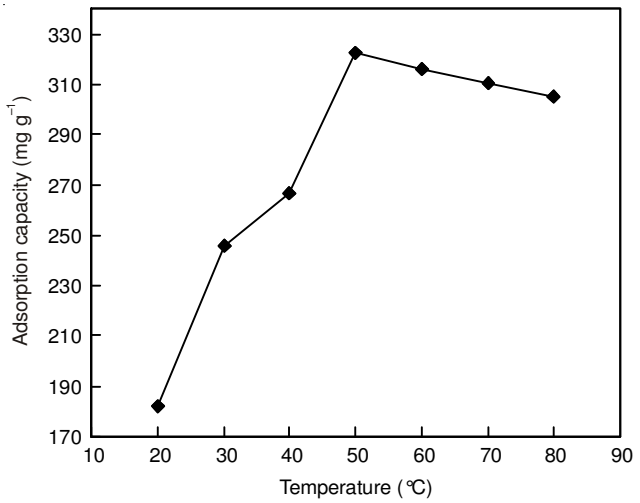

Fig. 3. Effect of temperature on adsorption capacity of lignocellulose/montmorillonite nanocomposite

Effect of time on adsorption: The effects of different adsorption times on lignocellulose/montmorillonite adsorption capacity are shown in Fig. 4. As indicated in Fig. 4, when the contact time was prolonged, the trend of adsorption capacity of the lignocellulose/montmorillonite towards Cu(II) increased rapidly at first and then dropped. This result may be considered that because of Cu(II) introduced to the adsorbent surface at a short contact time, which was then followed by spreading into the adsorbent microporous and finally forming a complex with the active sites of the adsorbent, so resulting in a sharply adsorption equilibrium. Therefore, the optimum adsorption time was selected as 60 min in this study.

Adsorption kinetics: Fig. 5 shows the effect of time on adsorption capacities of Cu(II) by lignocellulose/montmorillonite nanocomposite. As can be seen, q_t increased significantly with an increase with t (min) at the initial stage and dropped afterwards with a continuous increase at t (min). Until adsorption reached equilibrium after 60 min, the adsorption amount reaching the maximum value. This results is attributed to the adsorption of Cu(II) on lignocellulose/montmorillonite

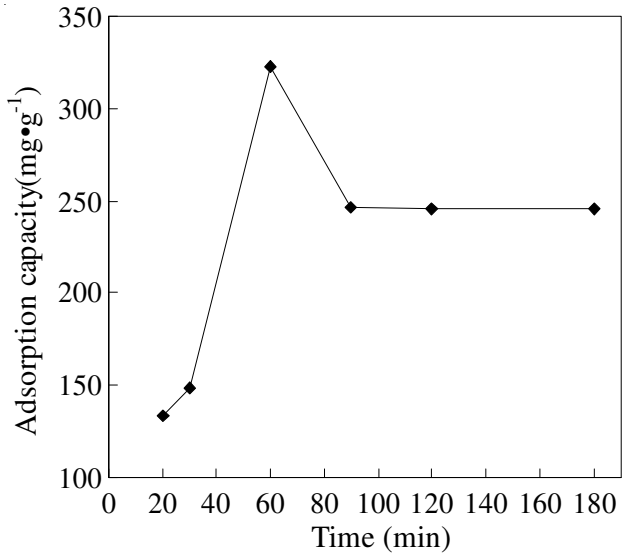

Fig. 4. Effect of reaction time on adsorption capacity of lignocellulose/montmorillonite nanocomposite

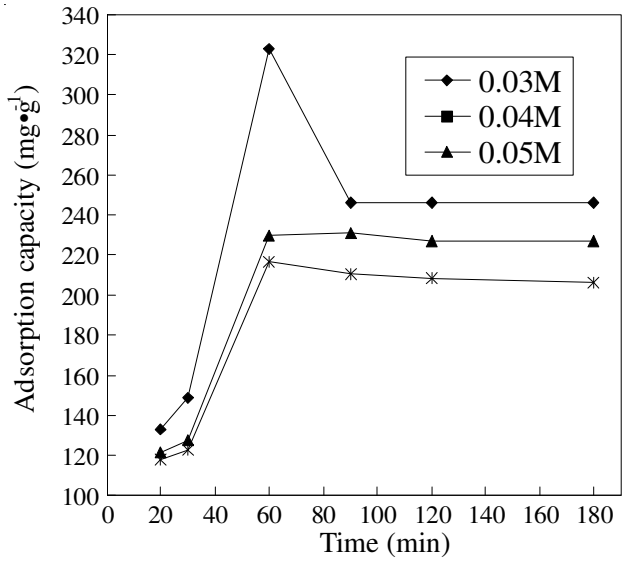

Fig. 5. Effect of different Cu(II) initial concentrations on adsorption efficiencies

as follows: firstly, the Cu(II) was adsorbed on the surface of the nanocomposite, where it could then react with the active groups, leading to an acceleration in adsorption rate, after that, the Cu(II) spread into the interior through surface microporous channels, which resulted in a decline in the adsorption rate. Finally, the adsorption equilibrium was reached.

The adsorption kinetic curve of the lignocellulose/montmorillonite was modeled by fitting the pseudo-first-order adsorption kinetics[18] eqn. 3 and the pseudo-second-order adsorption kinetics[19] eqn. 4.

$$\log (q_e - q_t) = \log q_e - \frac{k_1 t}{2.303} \quad (3)$$

$$\frac{t}{q_t} = \frac{1}{k_2 q_e^2} + \frac{t}{q_e} \quad (4)$$

Here, q_e(mg g^{-1}) stands for the amount of adsorption upon reaching equilibrium. q_t(mg g^{-1}) is the adsorption amount at time t (min). k_1(min^{-1}) is the rate constant of the pseudo-first-order adsorption kinetics equation. k_2[g(mg $min^{-1})^{-1}$] is the rate constant of the pseudo-second-order adsorption kinetics equation.

Results of adsorption kinetics and model fitting are presented in Table-1 and Fig. 6. For the adsorption process of the lignocellulose/montmorillonite, the fitting correlation coefficient (R^2) of the pseudo-second-order adsorption kinetics equation was higher than that of the pseudo-first-order equation. The adsorption amount obtained from experimental results at the state of equilibrium was close to that of the pseudo-second-order adsorption kinetics equation. This result indicates that the adsorption rate depends on the concentration of Cu(II) at lignocellulose/montmorillonite surface and the adsorbance of these adsorbed at equilibrium[20,21].

TABLE-1
KINETIC PARAMETERS OF Cu(II) ADSORPTION ONTO LIGNOCELLULOSE/MONTMORILLONITE

Models	q_e (mg g^{-1})	q_{ec} (mg g^{-1})	k	Correlation coefficient (R^2)
Pseudo-first order	322.56	162.26	0.0055	0.5613
Pseudo-second order	322.56	277.78	0.0002	0.9856

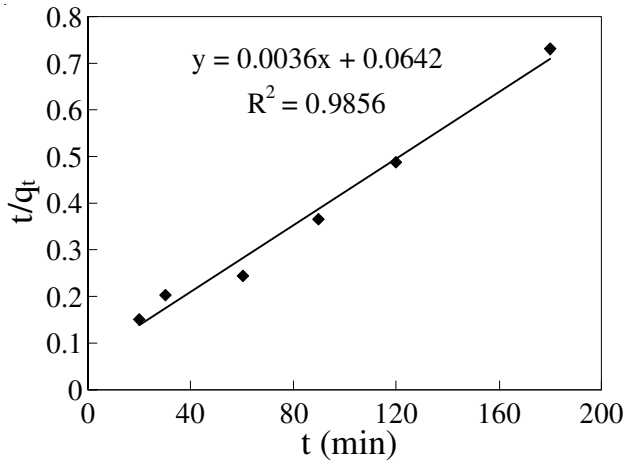

Fig. 6. Pseudo-second-order adsorption kinetics fitted equation of Cu(II) adsorption by lignocellulose/montmorillonite (T = 50 °C, initial concentration of Cu(II) = 0.03 mol L^{-1}, pH = 4.9)

Adsorption isotherms: Fig. 7 shows the adsorption capacity of Cu(II) by lignocellulose/montmorillonite at different Cu(II) concentrations at adsorption temperature of 40, 50 and 60 °C. Isothermal adsorption curves were plotted by using the equilibrium adsorption amount qe and adsorption equilibrium concentration C_e. Fig. 7 showed that the Cu(II) adsorption equilibrium amount on lignocellulose/montmorillonite was enhanced with an increase in the Cu(II) concentration. Moreover, the degree of increase was higher at a lower concentration and remained stable when Cu(II) concentration became higher. This could be attributed to the particular amount of active adsorption sites on lignocellulose/montmorillonite. At a low initial concentration, the adsorbent would have enough active adsorption sites to interact with Cu(II), however, after Cu(II) concentration reached a certain level, the active adsorption sites on the adsorbent surface were mostly occupied by Cu(II) ions, leading to the limitation of further adsorption, thus remaining a stable adsorption capacity.

Isothermal adsorption curves were fitted and plotted by employing the Langmuir eqn. 5 and Freundlich[22] eqn. 6:

$$\frac{C_e}{q_e} = \frac{1}{bq_{max}} + \frac{C_e}{q_{max}} \quad (5)$$

$$\ln q_e = \ln k_f + \frac{1}{n} \ln C_e \quad (6)$$

where b (L mg^{-1}) refers to the Langmuir constant, which relates to the adsorption capacity. n and k_f are Freundlich constants. C_e (mol L^{-1}) is the concentration of Cu(II) at equilibrium. q_{max} (mg g^{-1}) is the monolayer saturation adsorption. q_e (mg g^{-1}) is the adsorption capacity at equilibrium.

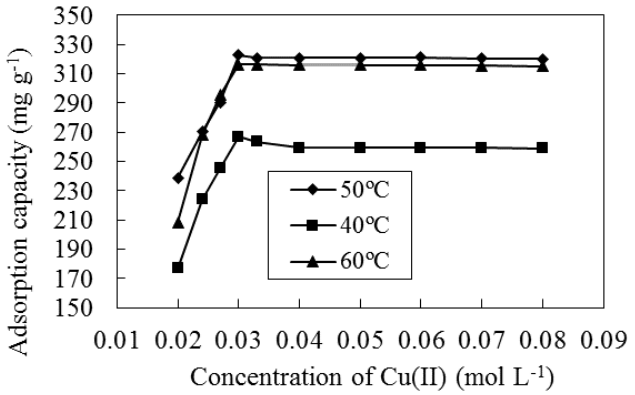

Fig. 7. Effect of temperature on adsorption efficiencies

Fitting results are presented in Table-2 and Fig. 8. From comparisons of the correlation coefficients (R^2) at T = 50 °C and pH = 4.9, it is observed that the adsorption of Cu(II) by the lignocellulose/montmorillonite was consistent with Langmuir isothermal adsorption models. The linear correlation coefficient R^2 was calculated as 0.9938, which indicates that the adsorption process belongs to the monolayer adsorption[23].

TABLE-2
ADSORPTION EQUILIBRIUM CONSTANT OBTAINED FROM LANGMUIR AND FREUNDLICH ISOTHERMS FOR Cu(II) ADSORPTION ONTO LIGNOCELLULOSE/MONTMORILLONITE

Langmuir model			Freundlich model		
q_{max}(mg g^{-1})	b	Correlation coefficient (R^2)	k_f	n	Correlation coefficient (R^2)
322.56	0.000147	0.9938	120.04	8.285	0.4411

Analysis of adsorption mechanism of lignocellulose/montmorillonite: The surface structure of the lignocellulose/montmorillonite is directly related to the adsorption of heavy metal ions. Scanning electron microscopy (SEM) was employed to characterize the surface microstructure of lignocellulose/montmorillonite and differences on the surface before and after the adsorption of heavy metal Cu(II) were analyzed. In order to determine the fundamental reason for the differences on lignocellulose/montmorillonite adsorption properties, FTIR analysis was conducted to further explore the active adsorption sites of lignocellulose/montmorillonite.

SEM analysis: Fig. 9 illustrates the SEM images of lignocellulose/montmorillonite before and after the adsorption of Cu(II). It can be seen from Fig. 9 that curly or irregular clusters of polymerized sheet-stacking dispersion appeared on the flat

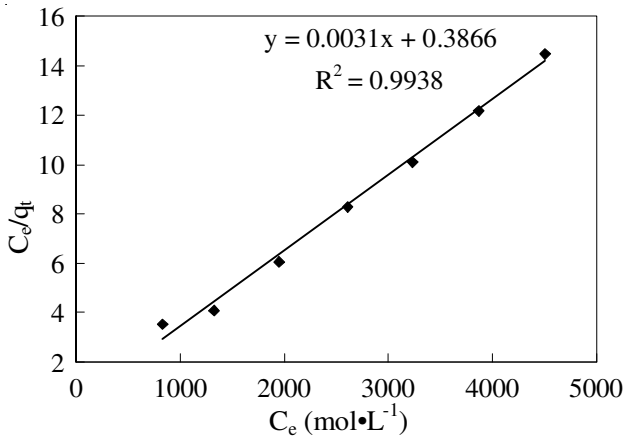

Fig. 8. Langmuir adsorption isotherm of Cu(II) adsorption by lignocellulose/montmorillonite (T = 50 °C, pH = 4.9, t = 60 min)

surface of lignocellulose/montmorillonite (Fig. 9a). These structures indicate that the lignocellulose reacted with the montmorillonite and the nanolamellar structure of montmorillonite was crushed and spread into the lignocellulose matrix due to the existence of microporous, which can enhance the contact areas for the adsorption of Cu(II). After the adsorption of Cu(II) (Fig. 9b), the lignocellulose/montmorillonite surface was evenly packed with Cu(II) and the sheet stacking structure was no longer apparent, indicating that the active sites used for adsorbing Cu(II) exist mainly on the protruding tip on surface. Copper(II) played a bridging role in as much as it connected surface active sites so that the surface became smooth, further indicating the strong interaction of Cu(II) with the adsorbent and demonstrating that the reaction process is mainly dominated by chemical adsorption[24].

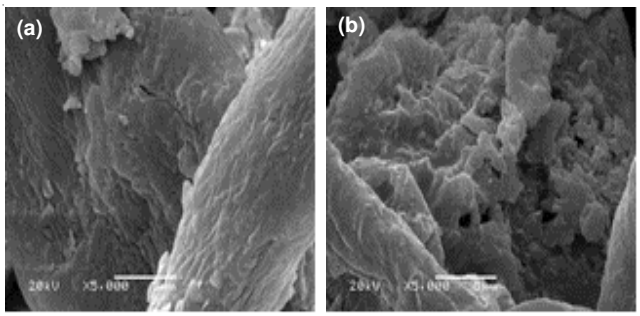

Fig. 9. SEM images of lignocellulose/montmorillonite before (a) and after (b) the adsorption of Cu(II)

FTIR analysis: Fig. 10a-c show the FTIR spectra of lignocellulose/montmorillonite, the nanoncomposite after desorption of Cu(II) and after adsorption of Cu(II), respectively. As seen in Fig. 10, the strong broad absorption peaks at 3464 cm^{-1} are attributed to the intramolecular O-H stretching vibration absorption peak as well as the characteristic absorption peak of intermolecular hydrogen bonding between phenol and alcohol molecules. The absorption peak shifted to a lower wavenumber at 3410 cm^{-1} after the adsorption of Cu(II), exhibiting a narrow peak in the spectrum, indicating that some of the O-H and corresponding hydrogen bonds were broken to react with Cu(II), this peak moved to 3438 cm^{-1} after desorption. The absorption peak at 2936 cm^{-1} represents the C-H stretching vibration associated with the aromatic ring. This

peak showed no obvious changes after adsorption and desorption of Cu(II). The strong broad absorption peak at 1732 cm^{-1} corresponds to the characteristic asymmetric stretch vibration of the C=O bond in carboxylic acids; this peak disappeared after adsorption of Cu(II) and appeared again after desorption of Cu(II) with a 1 cm^{-1} shift to a lower wavenumber (1731 cm^{-1}). The vibration absorption peak of the carboxyl O-H bond located at 1401 cm^{-1} disappeared after Cu(II) adsorption, appearing again at 1401 cm^{-1} after Cu(II) desorption. The absorption peak at 1313 cm^{-1}, which represents the stretching vibration absorption of the C-O bond in phenol, moved 1-2 cm^{-1} to a higher wavenumber after Cu(II) absorption and then shifted back down to 1313 cm^{-1} after Cu(II) desorption. Moreover, the strong absorption peak at 1139 cm^{-1} corresponding to the stretching vibration absorption of the C-O bond found in alcohols shifted to a higher wavenumber (1148 cm^{-1}) after the absorption of Cu(II) with a decrease in peak intensity and shifted down to 1136 cm^{-1} after the desorption of Cu(II). Based on the analysis above, it is observed that the H^+ of the hydroxyl and carboxyl groups of the lignocellulose/montmorillonite structure were substituted by Cu(II) after adsorption. Slight changes were observed in the corresponding vibration absorption peak intensities of the reactive functional groups, moreover, the adsorption peak values were also shifted. Furthermore, the FTIR spectrum of the absorbent after desorption of Cu(II) nearly coincided with that of the original nano-composite. Therefore, the basic structure and properties of the lignocellulose/montmorillonite remained relatively stable in the process of Cu(II) adsorption and desorption, which is suggestive of its application as an excellent renewable adsorbent.

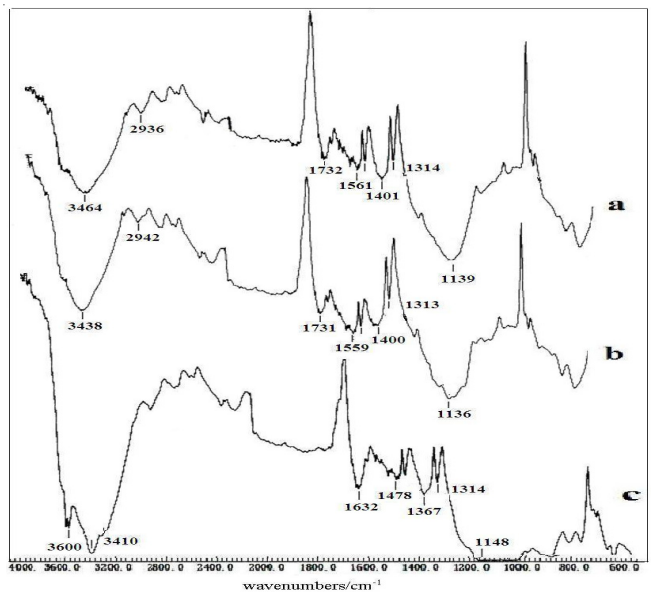

Fig. 10. FTIR spectra of lignocellulose/montmorillonite (a), after desorption of Cu(II) (b) and after adsorption of Cu(II) (c)

Influencing factors on Cu(II) desorption: The regeneration of an adsorbent after desorption is key to its economical desirability in practical applications[25]. Therefore, desorption properties of lignocellulose/montmorillonite saturated with adsorbed Cu(II) were investigated in this study. The effects of desorption reagent of HNO_3 concentration, desorption temperature and desorption time on the desorption capacity were studied.

Effect of HNO_3 concentration on desorption: The effects of different HNO_3 concentrations (0.1-0.5 mol L^{-1}) on Cu(II)-loaded lignocellulose/montmorillonite with respect to Cu(II) desorption capacity are shown in Fig. 11. It can be observed that Cu(II) desorption capacity of the lignocellulose/montmorillonite first increased and then decreased with an increase in HNO_3 concentration. This observation is likely because the increase in acid concentration would lead to the accumulation of H^+ in solution, thus increasing the concentration gradient of Cu(II) and H^+, resulting in an improvement in the driving force of ion exchange, which favors desorption. However, a high concentration of HNO_3 would dramatically increase the H^+ concentration in solution and thus enhance the electrostatic repulsion with Cu(II), which resulted in the inhibition of Cu(II) desorption[26]. Therefore, when the concentration of HNO_3 was set at 0.1 mol L^{-1}, the maximum desorption capacity of lignocellulose/montmorillonite reached 283.15 mg g^{-1}.

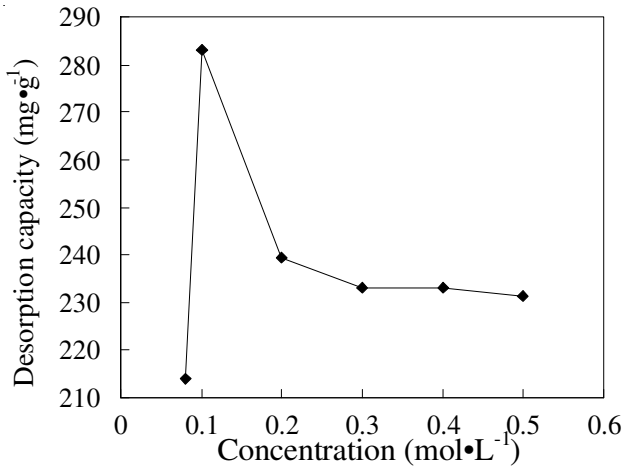

Fig. 11. Effect of HNO_3 concentration on desorption capacity of lignocellulose/montmorillonite nanocomposite

Effect of temperature on desorption: The effects of different desorption temperatures (30-80 °C) on Cu(II)-loaded lignocellulose/montmorillonite with in terms of Cu(II) desorption capacity are shown in Fig. 12. From Fig. 12, we can see that the Cu(II) desorption capacity of the lignocellulose/montmorillonite first increased and then decreased with an increase in desorption temperature. This decline in desorption is attributed to the partial damage of three dimensional structures of lignocellulose/montmorillonite, which decomposes at high temperature[27]. Therefore, the optimum desorption temperature was chosen as 40 °C.

Effect of time on desorption: The effects of different desorption times (10-60 min) on Cu(II) desorption capacity of Cu(II)-loaded lignocellulose/montmorillonite are shown in Fig. 13. Fig. 13 showed that the Cu(II) desorption capacity of the lignocellulose/montmorillonite first increased and then decreased with an increase in desorption time. This phenomenon is consistent with the occurrence of holes[28] produced by ultrasonic conditions. After a certain ultrasonic oscillation

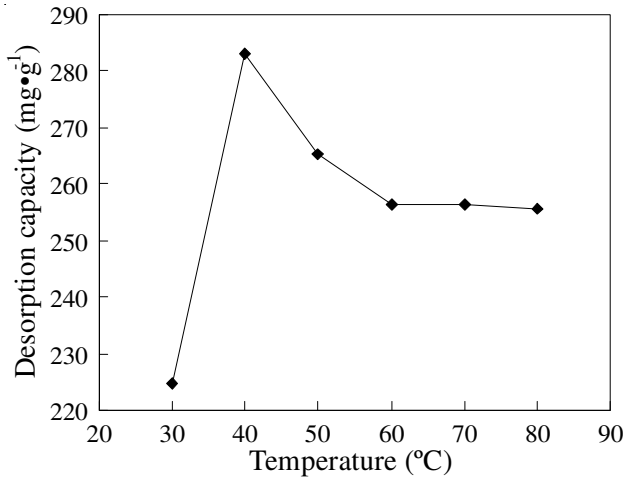

Fig. 12. Effect of temperature on desorption capacity of lignocellulose/montmorillonite nanocomposite

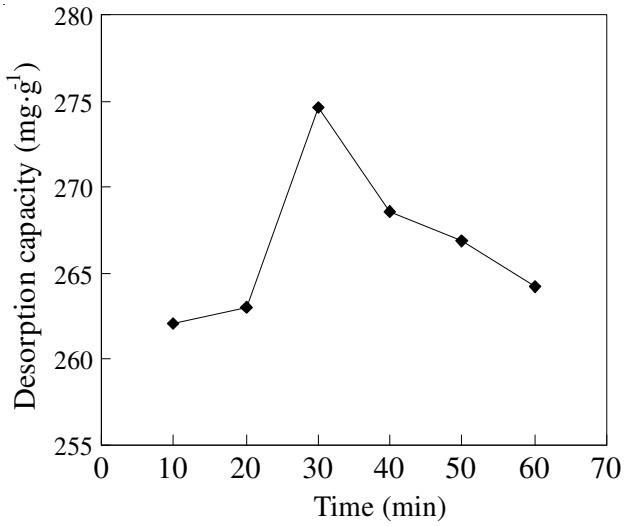

Fig. 13. Effect of time on desorption capacity of lignocellulose/montmorillonite nanocomposite

time, the concentration of holes in solution reached saturation. As shown in Fig. 13, lignocellulose/montmorillonite reached the maximum desorption amount after an ultrasonic desorption time of 0.5 h. lignocellulose/montmorillonite can potentially be regenerated and recycled.

Recycling and reusability of lignocellulose/montmorillonite: Reusing of lignocellulose/montmorillonite keeps the processing cost down and opens the possibility of recovering Cu(II) extracted from the wastewater. Thus recycling of lignocellulose/montmorillonite was a very important parameter for its practical application. To evalutate the reusability of lignocellulose/montmorillonite, the consecutive adsorption/desorption process was performed over 5 consecutive times. The effects of the number of lignocellulose/montmorillonite adsorption/desorption cycles on the Cu(II) adsorption/desorption capacity are shown in Table-3. These results suggested that the lignocellulose/montmorillonite can be recycled up to 4 times while retaining optimal adsorption/desorption conditions, the adsorption/desorption capacity for each process after the 4th cycle was found to be 309.57 and 252.44 mg g^{-1}, respectively. Therefore, this work has built a solid foundation for the practical application of lignocellulose/montmorillonite as an adsorbent for the removal of Cu(II) and indicated that lignocellulose/montmorillonite was a high performance, low-cost and recyclable green adsorbent for the wastewater treatment.

TABLE-3
LIGNOCELLULOSE/MONTMORILLONITE ADSORPTION/DESORPTION CAPACITIES FOR Cu(II) AFTER MULTIPLE CYCLES

Recycle times	1st	2nd	3rd	4th	5th
Adsorption Q_e (mg g^{-1})	322.56	319.42	320.50	309.57	238.15
Desorption Q_e (mg g^{-1})	283.15	270.20	262.53	252.44	177.06

Conclusions

A novel lignocellulose/montmorillonite nanocomposite has been prepared by intercalation. Lignocellulose/montmorillonite can be effectively applied in the adsorption Cu(II) ions in wastewater. The maximum adsorption capacity of the lignocellulose/montmorillonite for Cu(II) reached 322.56 mg g^{-1} under conditions corresponding to an initial Cu(II) concentration of 0.03 mol L^{-1}, pH of 4.9, adsorption temperature of 50 °C and adsorption time of 60 min. The adsorption kinetics and isotherms were fitted well to both the pseudo-second-order adsorption kinetics equation (R^2 = 0.9856) and Langmuir isothermal adsorption models (R^2 = 0.9938). These results indicate that the adsorption equilibrium was mainly dominated by monolayer chemical adsorption in the experimental range.

The effects on desorption capacity of Cu(II)-loaded lignocellulose/montmorillonite by using HNO_3 as a desorption agent in ultrasonic oscillation treatment. The optimum conditions of desorption were as follows: The concentration of HNO_3 was 0.1 moL L^{-1}, the temperature of desorption was 40 °C and the time of desorption was 0.5 h. Under the optimum conditions, the maximum desorption capacity was determined as 283.15 mg g^{-1}.

The adsorption/desorption experiments demonstrated that the adsorption and desorption capacity of lignocellulose/montmorillonite remained at a relatively high level after four adsorption/desorption recycling times. The study showed that lignocellulose/montmorillonite nanocomposite could be excellent potential for recycling to removal of Cu(II) from industrial wastewater.

ACKNOWLEDGEMENTS

This work was financially supported as part of the Special Funds for Forestry Research and Public Service Industry of China (No. 201104004) and the Science Foundation for College of the Inner Mongolia Autonomous Region (No. JC2012004).

REFERENCES

1. A. Demirbas, *J. Hazard. Mater.*, **157**, 220 (2008).
2. L.S. Li, Y.Z. Yang, H.S. Jia, L.Q. Yang, Q.F. Cao and X.G. Liu, *J. Chem. Ind. Eng.*, **64**, 3381 (2013).
3. D. Sud, G. Mahajan and M.P. Kaur, *Bioresour. Technol.*, **99**, 6017 (2008).
4. B. Acemioglu, A. Samil, M.H. Almai and R. Gundogan, *J. Appl. Polym. Sci.*, **89**, 1537 (2003).
5. V.K. Gupta, P.J.M. Carrott, M.M.L. Ribeiro Carrott and Suhas, *Crit. Rev. Environ. Sci. Technol.*, **39**, 783 (2009).
6. M. Sciban and M. Klasnja, *Adsorpt. Sci. Technol.*, **22**, 195 (2004).
7. D. Mohan, C.U. Pittman Jr. and P.H. Steele, *J. Colloid Interf. Sci.*, **297**, 489 (2006).
8. X.Y. Guo, S.Z. Zhang and X.Q. Shan, *J. Hazard. Mater.*, **151**, 134 (2008).
9. M.E. Argun, S. Dursun and K. Gur, *Cell. Chem. Technol.*, **39**, 581 (2005).

10. S. Babel and T.A. Kurniawan, *J. Hazard. Mater*., **97**, 219 (2003).
11. A. Fujimori, J.-I. Kusaka and R. Nomura, *Polym. Eng. Sci*., **51**, 1099 (2011).
12. R. Garcia-Valls and T.A. Hatton, *Chem. Eng. J*., **94**, 99 (2003).
13. L. Wang and F.L. Pang, *J. Funct. Polym*., **23**, 103 (2010).
14. K.M.M.K. Prasad and S. Raheem, *Mikrochim Acta.*, **112**, 63 (1993).
15. J.P. Zhang and A.Q. Wang, *J. Chem. Eng. Data*, **55**, 2379 (2010).
16. Y.F. Zhou and R.J.A. Haynes, *Water Air Soil Pollut*., **218**, 457 (2011).
17. X. Wen, L. Wu and H. Tang, *Bull. Environ. Contam. Toxicol*., **67**, 913 (2001).
18. K.V. Kumar and V.T. Favere, *Polymer*, **47**, 1772 (2006).
19. H. Demir, A. Top, D. Balkose and S. Ulku, *J. Hazard. Mater*., **153**, 389 (2008).
20. P. Ding, K.L. Huang, G.Y. Li, W.W. Zheng and F.P. Jiao, *Chem. Eur. J*., **7**, 503 (2006).
21. Y.S. Ho and G. Mckay, *Adsorpt. Sci. Technol*., **20**, 797 (2002).
22. K. Ramakrishnan and C. Namasivayam, *Toxicol. Environ. Chem*., **93**, 1111 (2011).
23. H.D. Doan, A. Lohi, V.B.H. Dang and T. Dang-Vu, *Process. Saf. Environ*., **86**, 259 (2008).
24. J.C. Zheng, H.M. Feng, M.H.W. Lam, P.K.S. Lam, Y.W. Ding and H.Q. Yu, *J. Hazard. Mater*., **171**, 780 (2009).
25. B.Y. Wang and K. Wang, *Bioresour. Technol*., **136**, 244 (2013).
26. H. Lalhruaitluanga, K. Jayaram, M.N.V. Prasad and K.K. Kumar, *J. Hazard. Mater*., **175**, 311 (2010).
27. L.M. Ottosen, H.K. Hansen and P.E. Jensen, *Water Air Soil Pollut*., **201**, 295 (2009).
28. W.X. Zheng and S.J. Wu, *Technol. Water. Treat*., **34**, 79 (2008).